.

Computational and experimental imaging of Mn defects on GaAs (110) cross-sectional surface

A. Stroppa,[1, 2, *] X. Duan,[1, 2, †] M. Peressi,[1, 2, ‡] D. Furlanetto,[3, 4] and S. Modesti[3, 4]

[1]*Dipartimento di Fisica Teorica, Università di Trieste,*

Strada Costiera 11, 34014 Trieste, Italy

[2]*CNR-INFM DEMOCRITOS National Simulation Center,*

via Beirut 2-4, 34014 Trieste, Italy

[3]*CNR-INFM TASC National Laboratory,*

Area Science Park, 34012 Trieste, Italy

[4]*Dipartimento di Fisica and Center of Excellence for Nanostructured Materials, CENMAT,*

Università di Trieste, via A. Valerio 2, 34127 Trieste, Italy

(Dated: February 1, 2008)

Abstract

We present a combined experimental and computational study of the (110) cross-sectional surface of Mn δ-doped GaAs samples. We focus our study on three different selected Mn defect configurations not previously studied in details, namely surface interstitial Mn, isolated and in pairs, and substitutional Mn atoms on cationic sites (Mn_{Ga}) in the first subsurface layer. The sensitivity of the STM images to the specific local environment allows to distinguish between Mn interstitials with nearest neighbor As atoms (Int_{As}) rather than Ga atoms (Int_{Ga}), and to identify the fingerprint of peculiar satellite features around subsurface substitutional Mn. The simulated STM maps for Int_{As}, both isolated and in pairs, and Mn_{Ga} in the first subsurface layer are consistent with some experimental images hitherto not fully characterized.

PACS numbers: 73.20.-r,73.43.Cd,68.37.Ef

I. INTRODUCTION

Mn-doped GaAs[1,2,3,4] has attracted considerable attention among the diluted magnetic semiconductors for its possible application in the emerging field of *spintronic*.[5,6,7] Although other materials such as ferromagnetic metals and alloys, Heusler alloys, or magnetic oxides seem to be promising candidates for spintronic devices, the diluted magnetic semiconductors and Mn-doped GaAs in particular are of tremendous interest in that they combine magnetic and semiconducting properties and allow an easy integration with the well established semiconductor technology. Besides possible spintronic applications, characterizing and understanding the properties of Mn defects in GaAs is a basic research problem which is still debated.

The growth conditions and techniques affect the solubility of Mn in GaAs, which is in general rather limited, and its particular defect configurations, thus determining the magnetic properties of the samples.[8,9,10,11,12] The highest Curie temperature T_c reachable for Mn-doped GaAs up to few years ago was 110 K,[13] rather low for practical technological purposes. Intense efforts have been pursued in the last years in order to understand the physics of this material and to improve its quality and efficiency. Out-equilibrium growth techniques[1,5] have enabled to increase the solubility of Mn and the Curie temperature; post-growth annealing of epitaxial samples at temperatures only slightly above the growth temperature has been particularly successfull.[9,10,14] Nowadays, δ-doping is used as an alternative to the growth of bulk $Mn_xGa_{1-x}As$,[15,16] allowing to obtain locally high dopant concentrations and, remarkably, an important enhancement of T_c, up to about 250 K.[17,18]

For further improvements it is essential to investigate the different configurations of Mn impurities and their effect on the magnetic properties of the system. The most common and widely studied Mn configuration is substitutional in the cation sites (Mn_{Ga}), with Mn acting as a hole-producing acceptor.[17] To a less extent, Mn can also occupy interstitial sites, in particular tetrahedral ones. In such a case, it is expected to strongly modify the magnetic properties, acting as an electron-producing donor and hence destroying the free holes and hindering ferromagnetism.[19]

Interstitials have not been fully characterized up to now, although their existence has been suggested in different situations.[8,9,10,11,14,20,21,22,23,24,25,26] For instance, the enhancement of the Curie temperature after post-growth annealing has been attributed to the reduction of

interstitial defects with their out diffusion towards the surface.[11] It has been suggested that interstitial sites are highly mobile and could be immobilized when adjacent to substitutional Mn_{Ga}, thus forming compensated pairs with antiferromagnetic coupling.[27] A first identification of interstitial Mn dates back to almost fifteen years ago by electron paramagnetic resonance (EPR).[20] Very recently EPR spectra from variously doped and grown samples of Mn-doped epitaxial GaAs have allowed to identify the presence of ionized Mn interstitials at concentrations as low as 0.5%, although not providing details about the specific local environment of the interstitial site.[28] Recent X-ray absorption near edge structure (XANES) and extended x-ray absorption fine structure (EXAFS) spectra in Mn δ-doped GaAs samples suggest that Mn occupy not only substitutional Ga sites but *also* interstitial sites, mainly in case of Be co-doping.[29]

Cross-sectional Scanning Tunneling Microscopy (XSTM) allows a direct imaging of the electronic states and can be used to characterize the impurities near the cleavage surface.[30] In recent years several XSTM studies of Mn-doped GaAs samples have been performed but without a complete consensus on the defects characterization.[22,31,32,33,34,35,36,37,38] We stress that most of XSTM studies mainly concern $Mn_x Ga_{1-x}As$ alloys and have identified mainly substitutional Mn defects. δ-doped samples have been investigated by Yakunin et al.,[35] who pointed out the advantage that in such samples it is easy to discriminate Mn related defects from other defects.

From the theoretical point of view, numerical works have been also focused mainly on the simulation of XSTM images of substitutional impurities on uppermost surface layers.[31,33,34,35] A complete and detailed investigation of interstitial impurities as they can appear on the exposed cleaved surface is still lacking thus preventing the possibility of a comprehensive interpretation of all the available experimental XSTM images.

Mn δ-doped (001) GaAs samples recently grown at TASC Laboratory in Trieste and analyzed with XSTM on the (110) cleavage surface have shown several Mn related features (see Fig. 1). Some of them have already be studied by other groups, like the asymmetric cross-like (or butterfly-like) structures marked by A in Fig. 1(a), attributed to Mn acceptors a few atomic layers below the surface.[34] Some other features, such those marked by B, or those of Fig 1(b), have not been yet assigned to specific Mn configurations. In order to identify the kind of Mn defects that cause them we have performed new density functional simulation of cross-sectional XSTM images focusing on three selected defect configurations

not yet fully studied, but whose presence cannot be excluded in real samples. In particular, we focus our attention on interstitial surface configurations, both individual as well as in pairs. We have also considered Mn_{Ga} on the first layer below the surface and compared all the simulations with the experimental maps.

II. EXPERIMENTAL DETAILS

Mn δ-doped samples were grown by molecular beam epitaxy on GaAs(001) in a facility which includes a growth chamber for III-V materials and a metallization chamber. After the growth of a Be doped buffer at 590°C and of an undoped GaAs layer 50 nm thick at 450°C with an As/Ga beam pressure ratio of 15, the samples were transferred in the metallization chamber where a submonolayer-thick Mn layer was deposited at room temperature at the rate of 0.003 monolayer/s. An undoped GaAs cap layer was subsequently grown at 450°C. This procedure was repeated in order to have three δ-doped Mn layer of 0.01, 0.05 and 0.2 monolayers in the same sample. During the transfers and the Mn deposition the vacuum was always better than 2×10^{-8} Pa. The 0.1 mm thick wafers containing the Mn layers were cleaved in situ in a ultra high vacuum STM system immediately prior to image acquisition to yield atomically flat, electronically unpinned {110} surfaces containing the [001] growth direction and the cross section of the δ-doped layer. The XSTM image presented in Fig. 1 and the others shown in this paper have been acquired from a δ-doped Mn layer of 0.2 monolayers with W tips.

The densities of the features observed by XSTM near each Mn layer were approximately proportional to the Mn coverage of the δ-doped layer in the range 0.01-0.2 monolayer. No trace of contaminants was observed by in situ x-ray photoemission spectroscopy after the transfer in the metallization, after the Mn deposition, and after the transfer in the growth chamber. For these two reasons we attribute the features observed by XSTM to the Mn atoms, and not to defects or contaminants caused by the growth interruption and transfers between the chambers. The density of the defects caused by these steps should not depend on the Mn coverage, contrary to what we observe. Moreover, a sample was grown with the same procedure described above, including the transfers between the chambers, but without the Mn deposition. The photoluminescence spectra of this sample are undistinguishable from that of a good undoped GaAs epitaxial layer grown without transfers between the chambers.

This confirms that the transfers do not introduce an appreciable amount of defects.

III.   THEORETICAL APPROACH

Our numerical approach is based on spin-resolved Density Functional Theory (DFT) using the *ab-initio* pseudopotential plane-wave method `PWscf` code of the *Quantum ESPRESSO* distribution.[39] Cross-sectional surfaces are studied using supercells with slab geometries, according to a scheme previously used,[40] with 5 atomic layers and a vacuum region equivalent to 8 atomic layers. Mn dopants are on one surface, whereas the other is passivated with hydrogen. For a single Mn impurity we use a 4×4 in-plane periodicity corresponding to distances between the Mn atom and its periodic images of 15.7 Å along the [1$\bar{1}$0] and 22.2 Å along [001]. No substantial changes in the XSTM images have been found using a 6×4 periodicity, which has been instead routinely used when considering interstitial complexes. Other details on technicalities can be found in Ref. 41.

In our study, we have mainly focused on the Local Spin Density Approximation (LSDA) for the exchange-correlation functional. An ultrasoft pseudopotential is used for Mn atom, considering semicore $3p$ and $3s$ states kept in the valence shell while norm-conserving pseudopotentials have been considered for Ga and As atoms. The 3d-Ga electrons are considered as part of core states.[42,43]

Tests beyond LSDA (with Generalized Gradient Correction and LSDA+U methods) have not shown any substantial difference in the features of the XSTM maps. As a further check, we have also simulated ionized substitutional Mn_{Ga} (with charge state equal to 1−) on surface and in the first subsurface layer as well as ionized interstitial Mn (with charge state equal to 2+) on surface layer. Neither the former nor the latter simulated XSTM maps show significant differences with respect to the neutral cases. We address the reader to a future pubblication for details.[44]

The XSTM images are simulated using the model of Tersoff-Hamann,[45,46] where the tunneling current is proportional to the Local Density of States (LDOS) at the position of the tip, integrated in the energy range between the Fermi energy E_f and $E_f + eV_b$, where V_b is the bias applied to the sample with respect to the tip. The position of the Fermi level is relevant for the XSTM images. In general, E_f strongly depends on the concentration of dopants: this is contrivedly large in our simulations even in the case of a single Mn dopant

per supercell. Therefore to overcome this problem we fix E_f according to the experimental indications: in order to account for the p-doping in the real samples, we set E_f close to the Valence Band Maximum (VBM). The VBM in the DOS of the Mn-doped GaAs can be exactly identified by aligning the DOS projected onto surface atoms far from the impurity with the one of the clean surface. In any case, the comparison between experiments and simulations must be taken with some caution, due to the possible differences in the details entering in the determination of the XSTM image, such as tip-surface separation, precise value of the bias voltage and position of E_f, surface band gap.[47]

IV. SURFACE MN INTERSTITIALS

We first focus on interstitial dopant configurations, Int_{As} and Int_{Ga}. Throughout this work we have considered only *tetrahedral* interstitial position, since it is known from bulk calculations that the total energy corresponding to the *hexagonal* interstitial site is higher by more than 0.5 eV.[11,48,49] The tetrahedral interstitial site in the ideal geometry has four nearest-neighbor (NN) atoms at a distance equal to the ideal host bond length d_1 and six next-nearest-neighbor (NNN) atoms at the distance $d_2 = \frac{2}{\sqrt{3}}d_1$, which are As(Ga) atoms for $Int_{Ga(As)}$, respectively. At the ideal truncated (110) surface, the numbers of NNs and NNNs reduce to three (2 surface atoms and 1 subsurface atom) and four (2 surface atoms and 2 subsurface atoms) instead of four and six respectively.

In the uppermost panels of Fig. 2 we show a ball and stick side and top view of the relaxed Int_{As} and Int_{Ga} configurations. In the relaxed structure, due to symmetry breaking because of the surface and the consequent buckling of the outermost surface layers, the NN and NNN bond lengths are no longer equal. Furthermore, some relaxed NNs bond lengths turn out to be longer than NNNs ones. In the following, we do not distinguish among NN and NNN atoms: they are simply referred as neighbor *surface* or *subsurface* atoms, as shown in the Figure.

The two relaxed configurations slightly differ in energy, by $\sim$ 130 meV/Mn atom, in favour of Int_{Ga}. This is at variance with the bulk case studied in the literature, where it has been found that Int_{As} is favoured: for neutral state, the energy difference is actually so small (5 meV/Mn atom)[48] that it is not meaningful, but it goes up to 350 meV in case of interstitial Mn with 2+ charge state.[11]

After optimization of the atomic positions, sizeable displacements from the ideal zinc blende positions occur for the Mn impurities and their surface and subsurface neighbors; small relaxations effects are still present in the third layer, in both configurations. In Int_{As}, with respect to the ideal (110) surface plane, Mn relaxes outward by ~ 0.06 Å and As_{surf} ($As_{subsurf}$) move upwards (downwards). On the other hand, the Ga atoms (both on surface and subsurface) are shifted towards the bulk. In Int_{Ga}, Mn relaxes inward by ~ 0.32 Å; the Ga_{surf} and $Ga_{subsurf}$ atoms are displaced downwards and the As_{surf} ($As_{subsurf}$) atom moves upwards (downwards). The interatomic distances between Mn and the nearest atoms are in general longer by more than 2-3 % than ideal values (details in Ref. 41).

The simulated XSTM images of Int_{As} (left) and Int_{Ga} (right) configurations at negative and positive bias voltages (from $-$ 2.0 V to $+2.0$ V) are shown in the lower panels of Fig. 2. In Int_{As}, Mn appears as an additional bright spot at negative bias voltage ($V_b = -1$ V), slightly elongated in the [001] direction and located near the center of the surface unit cell identified by surface As atoms. The As_{surf} atoms close to Mn appear less bright than the others. These features are similar changing V_b from -1 to -2 V.

In the empty states image at $V_b = 1$ V Mn appears again as an elongated bright spot. The underlying cation lattice is only barely visible at this bias voltage. The very bright XSTM feature originates from the Mn d minority states and a strong peak of Ga_{surf} majority states.[50] At $V_b = 2$ V, this feature is still well visible, as well as another region brighter than the underlying cationic sublattice in correspondence of As_{surf} atoms neighbor to Mn, suggesting a contribution coming from the hybridization between Mn-d and As_{surf}-p states.

In Int_{Ga} configuration, at negative voltage, Mn appears as an almost circular bright spot located in between two surface As atoms adjacent along the [001] direction. At positive bias voltages, the two Ga_{surf} atoms neighbor to Mn appear very bright with features extending towards Mn in a "v"-shaped form and the atoms in the neighborhood also look brighter than normal. These features remain visible by increasing the positive bias voltage up to 2 eV. Remarkably the empty states images of Mn are quite different for the two interstitial configurations, making them clearly distinguishable by XSTM analysis. Some features in the experimental XSTM images appear as bright spots both at positive and negative bias voltages. These spots lie along the [001] Ga rows and between the [1-10] Ga columns at positive bias voltage (see Fig. 1(b)). Their location with respect to the surface Ga lattice and the comparison with the simulated images allow to identify them as Int_{As} Mn atoms.

The numerical simulation gives easily informations on the magnetic properties of the system. The total and absolute magnetization, calculated from the spatial integration of the difference and the absolute difference respectively between the majority and minority electronic charge distribution, are different in the two configurations: 4.23 and 4.84 μ_B for Int_{As} and 3.41 and 4.71 μ_B for Int_{Ga} respectively. These differences indicate in both cases the presence of region of negative spin-density and a clear dependence of the induced magnetization on the local Mn environment. The individual atomic magnetic moments can be calculated as the difference between the majority and minority atomic-projected charges. In Int_{As}, Mn magnetic moment is 3.96 μ_B, almost integer, corresponding to the presence of a gap in the Mn-projected minority density of states. Mn magnetization is slightly lower in Int_{Ga} (3.67 μ_B). In both cases they are significantly larger compared to the bulk case, indicating a surface induced enhancement. The analysis of spin-polarization induced by interstitial Mn on its nearest neighbors shows in both cases an antiferromagnetic Mn–Ga coupling and a smaller ferromagnetic Mn–As coupling: more precisely, the magnetic moments induced on surface Ga atoms neighbors to Mn are equal to -0.14 and -0.17 μ_B in Int_{As} and Int_{Ga} respectively, whereas those induced on surface or subsurface As atoms neighbors to Mn are positive and at most equal to 0.05 μ_B. We address the reader to Ref.[41] for further details.

In the experimental images of Mn δ-doped GaAs samples we often observe two spots close one each other at a distance of about 8 Å, as reported in Fig. 3 (larger panel). The simulated image of two Int_{As} atoms separated by a clean surface unit cell along ($1\bar{1}0$), partially superimposed, reproduces the main features of this experimental image, and it is basically a superposition of images of individual Int_{As} (elongated bright spot each one, with major axis along the [001] direction, and a surrounding darker region).

V.   SUBSTITUTIONAL MN DEFECTS IN THE FIRST SUBSURFACE LAYER

Another typical feature present in the experimental XSTM maps is a bright spot visible at positive bias voltages with two satellite features forming a triangular structure, as shown in Fig. 1(a) (feature B) and in Fig. 4 in the lower panels. This feature seems similar to that caused by the arsenic antisite defect (As on Ga) in GaAs.[51,52] However in the arsenic antisite defects the satellites are visible only at negative sample bias, while the defect that we

observe in the Mn layers shows satellite only in the positive bias images. On the other hand there is a clear resemblance of the defect B (Fig. 1(a) and Fig. 4) with the simulated image of a substitutional Mn_{Ga} atom in the first subsurface layer shown in the panels partially superimposed to the experimental images. It can be seen at $V_b < 0$ a deformation of the surface As rows in correspondence of the Mn impurity below, and, even more remarkably, the peculiar satellite bright features on two neighboring surface As stoms at $V_b > 0$ giving rise to a triangular-shaped image. Therefore we attribute the defect B to substitutional Mn Ga atoms in the first subsurface layer.

Finally, we discuss our findings in comparison with some relevant results present in the literature. The comparison of our simulations with those of Sullivan et al.[33] is possible only for the isolated Mn_{Ga} in the first subsurface layer at negative bias voltage: in such a case the simulated images show similar features. The corresponding image at positive bias is not reported and other configurations are not comparable.

The XSTM imaging of substitutional Mn is reported with more details by Mikkelsen et al.,[31,32] where both the simulated maps for surface and subsurface Mn_{Ga} and the experimental ones attributed to this impurity configuration are shown at negative and positive bias, thus allowing for a more complete comparison. The images for Mn_{Ga} in the first subsurface layer have a good resemblance with ours, a part from the satellite features that we have identified at positive bias on neighbor As atoms which are not present in their images, neither in the simulated nor in the experimental one. More precisely, we notice that their simulated surface area is too small to make such satellite features visible. The simulated images for surface Mn_{Ga} are also similar to ours and, like ours, not corresponding to any experimental feature.[44] This leads to the conclusion that the presence of substitutional Mn in the first layer of the exposed surface is very unlikely.

Mikkelsen et al. reported also the simulation of surface interstitial Mn in their Fig. 3(d),[32] that according to our understanding on the basis of the symmetry planes should correspond to Int_{Ga}, although not explicitly indicated. Their images are similar to ours for the same configuration. They rule out the presence of interstitials since these images are not compatible with experiments, at variance with our findings concerning Int_{As}. It should be noted however that we observe the Int_{As} features in the experimental samples only in the first few hours after the sample cleavage. They disappear for longer times, probably because of surface contamination or diffusion.

Kitchen et al.[36,37] report experimental images for Mn adatoms at the GaAs (110) surface with highly anisotropic extended star-like feature, attributed to a single surface Mn acceptor. Interestingly, these images are compatible with our simulated surface Mn_{Ga}, not show here.[44] A resemblance with our empty state image for Int_{As} (see Fig. 2 at V_b=+2 V) is instead only apparent because the mirror symmetry plane is different.

An anisotropic, crosslike feature in XSTM image is reported also Yakunin et al.[34] and, from comparison with an envelope-function, effective mass model and a tight-binding model, it is attributed to a hole bound to an individual Mn acceptor lying well below the surface. We observe similar feature of different sizes (see Fig. 1), the smallest of them are those reported in Fig. 4, that we identify as Mn_{Ga} in the first subsurface layer.

A part from different details, our simulated images for surface and subsurface Mn_{Ga} are compatible with such crosslike features, although experimental and simulated images reported therein concern substitutional impurities located more deeply subsurface than those we have considered. Crosslike features are observed even at very short Mn-Mn spatial separations.[35]

VI. CONCLUSIONS

We have reported a combined experimental and first-principles numerical study of XSTM images of the (110) cross-sectional surfaces of Mn δ-doped GaAs samples. We suggest an identification of three typical configurations observed in the experimental sample on the basis of a comparison of numerical prediction and observed images both at negative and positive applied bias. (i) Some structures observed can be identified as surface Mn interstitial with As nearest neighbors, on the basis of their position with respect to the surface lattice and the comparison with the simulated images. At variance, there is no evidence in the experimental samples of Mn interstitial with Ga nearest neighbors, whose XSTM imaging according to our numerical simulations would correspond to very different features. (ii) Besides isolated configurations, also pairs of Mn interstitials with As nearest neighbors are clearly observed and identified. (iii) Subsurface substitutional Mn_{Ga} atoms in the first subsurface layer can also be unambiguously identified in the experimental images by a main bright spot corresponding to the dopant and from peculiar satellite features on two neighboring As atoms which are clearly observed in the experimental images and predicted

by simulations.

VII. ACKNOWLEDGMENTS

* Electronic address: astroppa@ts.infn.it; Presently at: Institute of Material Physics, University of Vienna, Sensengasse 8/12, A-1090 Wien, Austria and Center for Computational Materials Science (CMS), Wien, Austria

† Presently at School of Physics, The University of Sydney, NSW 2006 Australia

‡ Electronic address: peressi@ts.infn.it

[1] K. Takamura et al., J. Appl. Phys. **89**, 7024 (2001).

[2] H. Ohno, A. Shen, F. Matsukura, A. Oiwa, A. Endo, S. Katsumoto, and Y. Iye, Appl. Phys. Lett. **82**, 3020 (2003).

[3] H. Ohno, F. Matsukura, and Y. Ohno, Mater. Sci. Eng. B **84**, 70 (2001).

[4] T. Jungwirth, Jairo Sinova, J. Mašek, J. Kučera and A.H. MacDonald, Rev. Mod. Phys. **78**, 809 (2006).

[5] H. Ohno, Science **281**, 51 (1998), and references therein.

[6] Y. Ohno, D.K. Young, B. Beschoten, F. Matsukura, H. Ohno, and D.D. Awschalom, Nature **402**, 790 (1999).

[7] H. Ohno, D. Chiba, F. Matsukura, T. Omiya, E. Abe, T. Dietl, Y. Ohno, and K. Ohtani, Nature **408**, 944 (2000).

[8] K.M. Yu, W. Walukiewicz, T. Wojtowicz, I. Kuryliszyn, X. Liu, Y. Sasaki, J.K. Furdyna, Phys. Rev. B **65**, 201303(R) (2002).

[9] K. W. Edmonds, K. Y. Wang, R. P. Campion, A. C. Neumann, N. R. S., Rarley, B. L. Gallagher, and C. T. Foxon, Appl. Phys. Lett. **81**, 4991 (2002).

[10] K. C. Ku, S. J. Potashnik, R. F. Wang, S. H. Chun, P. Schiffer, N. Samarth, M. J. Seong, A. Mascarenhas, E. Johnston-Halperin, R. C. Mayers, A. C. Gossard, and D. D. Awschalom, Appl. Phys. Lett. **82**, 2302 (2003).

[11] K.W. Edmonds, P. Boguslawski, K.Y. Wang, R.P. Campion, S.N. Novikov, N.R.S. Farley, B.L. Gallagher, C.T. Foxon, M. Sawicki, T. Dietl, M.B. Nardelli, and J. Bernholc, Phys. Rev. Lett. **92**, 037201 (2004).

[12] L. Bergqvist, P. A. Korzhavyi, B. Sanyal, S. Mirbt, I. A. Abrikosov, L. Nordström, E.A. Smirnova, P. Mohn, P. Svedlindh, and O. Eriksson, Phys. Rev. B **67**, 205201 (2003).

[13] F. Matsukura, H. Ohno, A. Shen, Y. Sugawara, Phys. Rev. B **57**, R2037 (1998).

[14] T. Jungwirth, K. Y. Wang, J. Mašek, K. W. Edmonds, Jürgen König, Jairo Sinova, M. Polini, N. A. Goncharuk, A. H. MacDonald, M. Sawicki, A. W. Rushforth, R. P. Campion, L. X. Zhao, C. T. Foxon, and B. L. Gallagher, Phys. Rev. B **72**, 165204 (2005).

[15] A.M. Nazmul, S. Sugahara, and M. Tanaka, Phys. Rev. B **67**, 241308(R) (2003).

[16] E. F. Schubert, J. M. Kuo, R. F. Kopf, H. S. Luftman, L. C. Hopkins, and N. J. Sauer, J. Appl. Phys. **67**, 1969 (1990).

[17] T. Dietl, H. Ohno, F. Matsukura, J. Cibert, and D. Ferrand, Science **287**, 1019 (2000).

[18] A.M. Nazmul, T. Amemiya, Y. Shuto, S. Sugahara, and M. Tanaka, Phys. Rev. Lett. **95**, 017201 (2005).

[19] P. Mahadevan and A. Zunger, Phys. Rev. B **68**, 075202 (2003).

[20] S.J.C.H.M. van Gisbergen, M. Godlewski, T. Gregorkiewicz, and C.A.J. Ammerlaan, Appl. Surf. Sci. **50**, 273 (1991).

[21] F. Glas, G. Patriarche, L. Largeau, and A. Lemaitre, Phys. Rev. Lett. **93**, 086107 (2004).

[22] G. Mahieu, P. Condette, B. Grandidier, J. P. Nys, G. Allan, D. Stivenard, Ph. Ebert, H. Shimizu, and M. Tanaka, Appl. Phys. Lett. **82**, 712 (2003).

[23] K. W. Edmonds, N. R. S. Farley, T. K. Johal, G. van der Laan, R. P. Campion, B. L. Gallagher, and C. T. Foxon, Phys. Rev. B **71**, 064418 (2005).

[24] R. Wu, Phys. Rev. Lett. **94**, 207201 (2005).

[25] S.C. Erwin and A.G. Petukhov, Phys. Rev. Lett. **89**, 227201 (2002).

[26] V. Holý, Z. Matěj, O. Pacherová, V. Novák, M. Cukr, K. Olejnik, and T. Jungwirth, Phys. Rev. B **74**, 245205 (2006).

[27] J. Blinowski, P. Kacman, Phys. Rev. B **67**, 121204(R) (2003).

[28] T. Weiers, Phys. Rev. B **73**, 033201 (2006).

[29] F. d'Acapito, G. Smolentsev, F. Boscherini, M. Piccin, G. Bais, S. Rubini, F. Martelli, and A. Franciosi, Phys. Rev. B **73**, 035314 (2006).

[30] R. M. Feenstra, Semicond. Sci. Technol. **9**, 2157 (1994).

[31] A. Mikkelsen, B. Sanyal, J. Sadowski, L. Ouattara, J. Kanski, S. Mirbt, O. Eriksson, and E. Lundgren, Phys. Rev. B **70**, 85411 (2004).

[32] A. Mikkelsen, E. Lundgren, Progress in Surf. Sci. **80**, 1 (2005).

[33] J. M. Sullivan, G. I. Boishin, L. J. Whitman, A. T. Hanbicki, B. T. Jonker, and S. C. Erwin, Phys. Rev. B **68**, 235324 (2003).

[34] A.M. Yakunin, A.Y. Silov, P.M. Koenraad, J.H. Wolter, W. Van Roy, J. De Boeck, J.M. Tang, M.E. Flatté, Phys. Rev. Lett. **92**, 216806 (2004).

[35] A.M. Yakunin, A.Yu. Silov, P.M. Koenraad, J.-M. Tang, M.E. Flatté, W. Van Roy, J. De Boeck, J.H. Wolter, Phys. Rev. Lett. **95**, 256402 (2005).

[36] D. Kitchen, A. Richardella, A. Yazdani, J. Supercond. **18**, 23 (2005).

[37] D. Kitchen, A. Richardella, J. Tang, M.E. Flattè, and A. Yazdani, Nature **442**, 436 (2006).

[38] J.N. Gleason, M.E. Hjelmstad, V.D. Dasika, R.S. Goldman, S. Fathpour, S. Charkrabarti, and P.K. Bhattacharya, Appl. Phys. Lett. **86**, 011911 (2005).

[39] http://www.pwscf.org and http://www.quantum-espresso.org

[40] X. Duan, M. Peressi, and S. Baroni, Phys. Rev. B **72**, 085341 (2005); X. Duan, S. Baroni, S. Modesti, and M. Peressi, Appl. Phys. Lett. **88**, 022114 (2006).

[41] A. Stroppa and M. Peressi, Mat. Sci. Eng. B **126** 217 (2006).

[42] Norm-conserving pseudopotentials from the publicly available *Quantum ESPRESSO* table are used: As.pz-bhs.UPF, Ga.pz-bhs.UPF, H.pz-vbc.UPF, and the pseudopotential for Mn used in Ref. 43

[43] A. Debernardi, M. Peressi, and A. Baldereschi, Mat. Sc. Eng. C **23**, 743 (2003) and other more recent works.

[44] A. Stroppa and M. Peressi, to be published.

[45] J. Tersoff and D.R. Hamann, Phys. Rev. Lett. **50**, 1998 (1983).

[46] J. Tersoff and D.R. Hamann, Phys. Rev. B **31**, 805 (1985).

[47] However, we have checked that a variation of $\sim \pm 0.3$ eV in the bias voltage considered in the simulated images does not affect their basic features.

[48] J. Mašek and F. Máca, Phys. Rev. B **69**, 165212 (2004).

[49] J.X. Cao, X.G. Gong, and R.Q. Wu, Phys. Rev. B **72**, 153410 (2005).

[50] A. Stroppa, Nuovo Cim. **29**, 315 (2006).

[51] R.M. Feenstra, J.M. Woodall and G.D. Pettit, Phys. Rev. Lett. **71**, 1176 (1993).

[52] G. Mathieu et al., Appl. Phys. Letters **82**, 712 (2003).

[53] A. Kokalj, Comp. Mater. Sci., 2003, Vol. 28, p. 155. Code available from http://www.xcrysden.org/.

FIG. 1: (a) Experimental (110) XSTM image of a 0.2 monolayer Mn δ-doped layer in GaAs at a sample bias voltage of 1.7 eV. This image has not been corrected for the drift of the sample. (b) XSTM image of a Mn related structure at the bias voltage of -1.4 eV (left) and $+1.9$ eV (right). The white lines show the [001] Ga atomic rows.

FIG. 2: Isolated Mn interstitial dopants on GaAs(110) surface, with As nearest neighbors (Int_{As}, left) and Ga nearest neighbors (Int_{Ga}, right). Upper panels: ball-and-stick model of the relaxed surface, top and side view. Only the three topmost layers are shown in the side view. Black spheres are Mn, white spheres are As, grey spheres are Ga. Lower panels: simulated XSTM images at occupied states and empty states respectively, for different bias voltages.

FIG. 3: Smaller superimposed panel: simulated XSTM image of a pair of Int_{As} on GaAs(110) surface with a relative distance of ~ 8 Å along the [1$\bar{1}$0] direction at a bias voltage $V_b = -2$ V. The larger panel shows an experimental image compatible with the simulation.

FIG. 4: Upper smaller superimposed panels simulated XSTM image of a subsurface Mn_{Ga} on GaAs(110) at negative (left) and positive (right) bias voltages. The lower panels show corresponding experimental images of the structure B (see Fig. 1(a)) taken at sample bias voltages of -1.4 V (left) and $+1.8$ V (right) that are compatible with the simulations, performed with voltages of -1 V and $+1$ V.
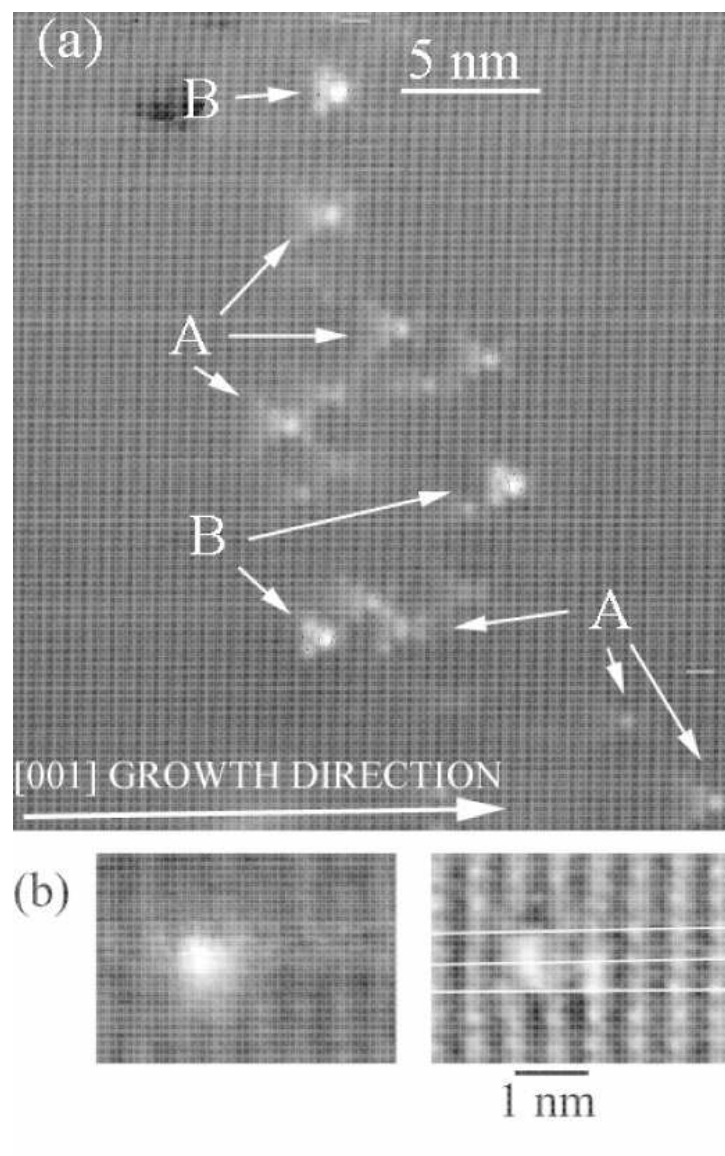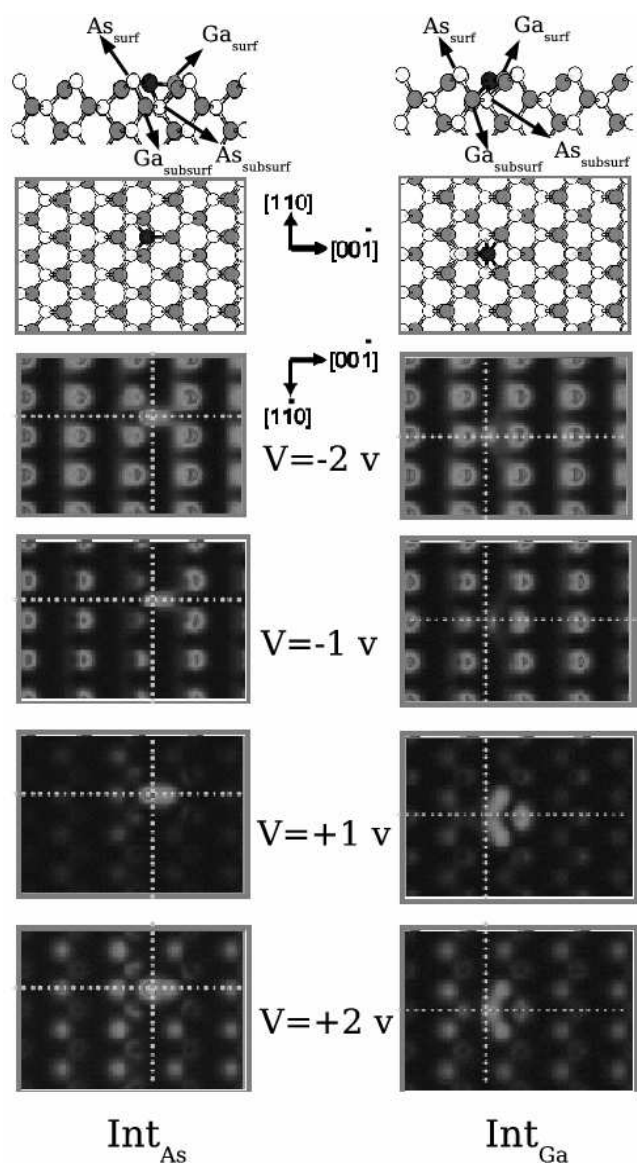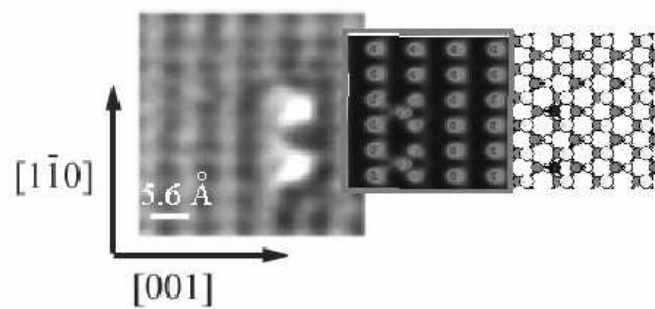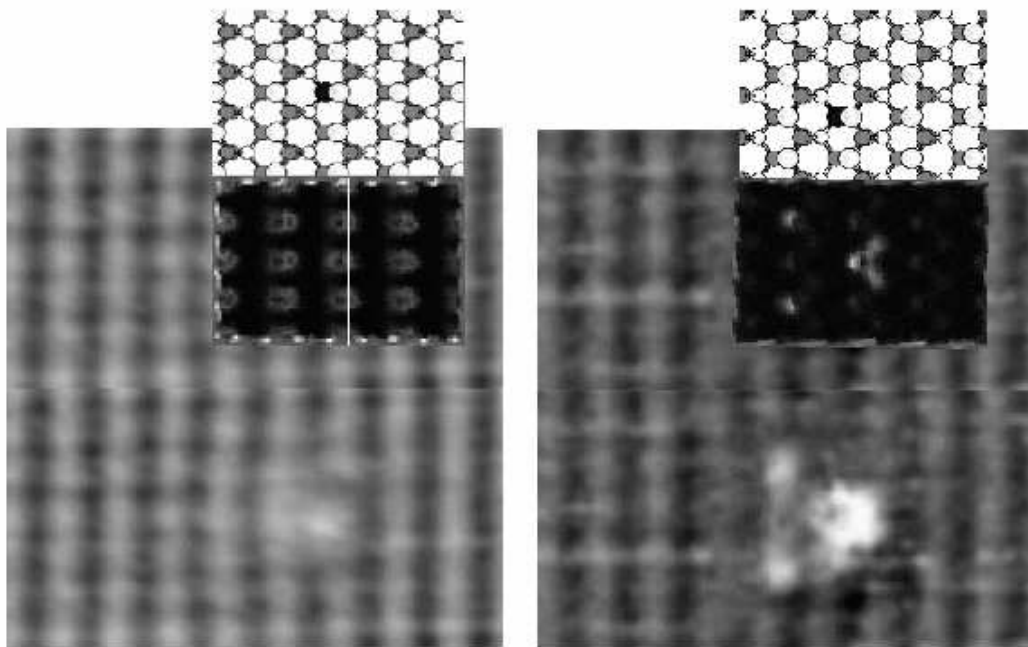
(a) 5 nm

B →

A →

B

A

[001] GROWTH DIRECTION

(b)

1 nm

Fig. 1

As$_{surf}$ Ga$_{surf}$ As$_{surf}$ Ga$_{surf}$

Ga$_{subsurf}$ As$_{subsurf}$ Ga$_{subsurf}$ As$_{subsurf}$

[110]
[001]

[001]
[110]
V=-2 v

V=-1 v

V=+1 v

V=+2 v

Int$_{As}$ Int$_{Ga}$

Fig. 2

$[1\bar{1}0]$

5.6 Å

$[001]$

Fig. 3

Fig. 4